Monte Carlo Simulations of Amphiphilic Co-Dendrimers in Dilute Solution

Ronan Connolly,[†] Edward G. Timoshenko,*[,‡] and Yuri A. Kuznetsov[§]

Theory and Computation Group, Department of Chemistry, Centre for Synthesis and Chemical Biology, Conway Institute of Biomolecular and Biomedical Research, and Centre for High Performance Computing Applications, University College Dublin, Belfield, Dublin 4, Ireland

Received February 23, 2004; Revised Manuscript Received July 1, 2004

ABSTRACT: Single−chain Monte Carlo simulations of amphiphilic diblock dendritic copolymers (co-dendrimers) with single and binary trifunctional cores were carried out in continuous space using implicit solvent. Two distinct topologies were studied: dendrimers with the hydrophobic blocks attached to the core, and dendrimers with the polar blocks attached to the core. Both topologies were found to be capable of forming micellar-type structures. As well as in terms of simulation snapshots, the systems were quantitatively compared via asphericity characteristics, monomer density profiles, mean-squared distances of monomers from the center of mass, and mean-squared bond lengths. Increasing the number of generations or increasing the number of spacers between branch points both yielded more well-defined shapes. Although increasing the number of generations of branching initially resulted in more spherical conformations (as for homodendrimers), it was found that high generation co-dendrimers adopted elongated cigar-like conformations for the single core case and dumbbell-like conformations for the binary core case. This phenomenon appears to involve the dendron segregation which occurs at the core of these large co-dendrimers.

1. Introduction

Dendritically branched polymers (dendrimers) are highly branched and reactive three-dimensional macromolecules, with all bonds originating from a central core.[1] These aesthetically pleasing synthetic macromolecules differ from standard polymers in two main ways. First, they are constructed from AB_n monomers (where n is typically either 2 or 3) instead of the standard AB monomers which produce linear polymers; i.e., each monomer in a dendrimer contains a branch point. Second, they are synthesized in an iterative fashion, with each successive iteration leading to increasing "generations" or layers of branching.

Because of their monodisperse nature, the large number of peripheral functionalities as well as the high degree of control over their structure, dendrimers are promising vectors for drug delivery. A review of the use of dendrimers as gene and drug delivery agents was recently carried out by Liu and Fréchet.[2] Many drug molecules synthesized by medicinal chemists tend to be quite hydrophobic (due to the large numbers of C and H atoms). This can be quite problematic for delivering drugs to the desired site of action, as it typically involves traveling through aqueous solutions (such as the bloodstream).[2−4] One approach to dealing with this problem is to synthesize water-soluble derivatives of the drug. Unfortunately, even small structural changes can often reduce the efficiency of the drug.[3] Another alternative is the use of drug delivery vectors. Micellar systems in aqueous solution dissolve the drug molecules within their hydrophobic interior, while the polar exterior of the micelle provides enough water solubility to dissolve the entire micelle.[2−4] The size of micelles generally ranges from 20 to 100 nm, and recognition by reticuloendothelial systems (a main reason for the premature removal of particles from the bloodstream) is considerably reduced for particles smaller than 100 nm in diameter. This increases the blood circulation time of the particles, which is desirable.[2,4] For these reasons, conventional polymeric micelles made from amphiphilic block copolymers have been studied as drug delivery vehicles.[5] Polymeric micelles are more stable than similar surfactant micelles. However, they still suffer from stability problems because they are only thermodynamically stable above the critical micelle concentration (cmc). When the concentration drops below the cmc, the micellar structure becomes unstable and dissociates into free chains. Thus, when the micellar vehicles are introduced into the human body, they are highly diluted below the cmc, becoming thermodynamically unstable. This could lead to disruption of the micellar structures, releasing the entrapped drugs prematurely.[2,4] In contrast, amphiphilic co-dendrimers can form so-called "unimolecular micelles",[2,4,6,7] where the amphiphilic copolymer "segments" are covalently attached to each other. Therefore, the micellar structure is static rather than dynamic in character, and it is maintained at all concentrations and in a variety of solvents.

Another advantage of dendrimers in drug delivery is the large number of end groups which can be functionalized, potentially allowing the introduction of specific target recognition groups to the vectors. The use of amphiphilic co-dendrimers as drug delivery vectors is being evaluated by several groups.[2,3,6,8] However, the authors have been unable to find any substantial

* To whom correspondence should be addressed. E-mail: edward.timoshenko@ucd.ie. http://darkstar.ucd.ie.

[†] Theory and Computation Group, Department of Chemistry, University College Dublin. E-mail: Ronan.Connolly@ucd.ie.

[‡] Theory and Computation Group, Centre for Synthesis and Chemical Biology, Conway Institute of Biomolecular and Biomedical Research, Department of Chemistry, University College Dublin. E-mail: Edward.Timoshenko@ucd.ie.

[§] Centre for High Performance Computing Applications, University College Dublin. E-mail: Yuri.Kuznetsov@ucd.ie.

10.1021/ma049638b CCC: $27.50
Published on Web 08/24/2004

theoretical or simulational evaluation of the properties of these systems.

The well-defined structures adopted by dendrimers also makes them promising building blocks in supramolecular chemistry (see ref 9 for a review of some current applications of dendrimers in this field). For these purposes, well-defined, "shape-persistent architectures"[10] are obviously very desirable. As well as the highly spherical structures adopted by flexible homodendrimers,[11] there is also interest in obtaining well-defined, nonspherical structures.[12,13] By using more than one type of monomer, i.e., co- (or hetero-) dendrimers, it should be possible to design different novel structures from dendrimers.

For both of these reasons, we feel that a detailed study of the conformations adopted by amphiphilic co-dendrimers in solution is necessary. We have recently studied the conformations adopted by dendritic homopolymers (homodendrimers) under different solvent conditions, using single-chain Monte Carlo simulations in continuous space,[11] and it seems natural to extend this study to include those of amphiphilic co-dendrimers.

2. Nomenclature Used

We will adopt essentially the same notation that we have previously used for describing homodendrimers.[11] Hence, we shall consider a dendrimer as consisting of G generations, each of which is separated by D spacers (with $D = 1$ corresponding to the case of each monomer being a branch point), with an F_0 functional core (corresponding to the generation $G = -1$) and all the other branch points of functionality F. For simplicity, we treat each monomer as an identical sphere of diameter $d^{(0)}$, but we distinguish between solubilities of different chemical repeating units. Also, increasing the number of spacers between branch points is equivalent to increasing the flexibility of the dendrimers, thus giving us some distinction between different dendrimers of the same generation. Very high values of D would correspond to recently synthesized dendritically branched star (or "hyperbranched") polymers.[14]

If $D = a$ and $G = b$, we shall denote such a dendrimer as DaGb, as in refs 11 and 15. The total number of monomers, N, will be

$$N = 1 + F_0 D \frac{(F-1)^{G+1} - 1}{F - 2} \tag{1}$$

For comparison with our earlier study of homodendrimers, we will mainly consider the case where all branch points have a functionality of 3, i.e., F, $F_0 = 3$. However, in terms of the literature,[2,4,6,7] the majority of currently synthesized amphiphilic co-dendrimers tend to possess tetrafunctional cores. Typically, a "binary core" is used, whereby two trifunctional cores are joined together to give an effective functionality of 4, i.e., $F_0 = 4$. Hence, we will also briefly consider the binary core case.

Because of the high symmetry of dendrimers, it is convenient to average monomer−monomer pairs over their symmetry equivalent classes. Hence, as for homodendrimers,[11] we will describe monomers in terms of their shell radial index, ρ, or "span", i.e., the number of bonds separating a monomer from the core monomer.

Typically, co-dendrimers are synthesized with a different outer shell from the rest of the dendrimer.[2−4,6,7] For example, hydrophilic poly(propyleneimine) dendrimers have been terminated by hydrophobic alkyl chains,[7d] and hydrophobic cores built from 4,4-bis(4′-hydroxyphenyl) pentanol have been coupled to polar poly(ethylene glycol) mesylate.[4] Therefore, we will distinguish two types of co-dendrimers, one where the hydrophobic (H) monomers are in the outermost generation and the rest of the monomers are polar (P), "outer-H", and the opposite case, "inner-H" (using a similar nomenclature to our previous studies of amphiphilic star copolymers).[16,17] Note that since the number of monomers, N, of these dendrimers approximately doubles with each generation, the inner-H and outer-H dendrimers described here have a composition of approximately $N_H/N \simeq 0.5$, where N_H is the number of H monomers.

Although the dendrimers are highly symmetrical polymers, it can be instructive to distinguish between monomers in distinct "dendrons". In convergent synthesis, dendrons are attached to a single core monomer to form a dendrimer.[1] Hence, we can consider the dendrimers discussed here as comprising three identical dendrons attached to a single core monomer, as illustrated in Figure 1.

3. Simulation Techniques

Monte Carlo (MC) simulations were carried out using the standard Metropolis algorithm.[18,19] All simulations were carried out in continuous space to avoid producing any lattice artifacts, which can be particularly problematic for highly branched systems as discussed in refs 11, 16, and 17, such as the dendrimers studied here.

We use the force field that we have previously used for studying amphiphilic star copolymers[16,17] and homodendrimers;[11] i.e., the Hamiltonian of the system is

$$\frac{H}{k_B T} = \frac{1}{2\ell^2}\sum_{i\sim j}\kappa_{ij}(\boldsymbol{X}_i - \boldsymbol{X}_j)^2 + \frac{1}{2}\sum_{ij,i\neq j} U_{ij}^{(LJ)}(|\boldsymbol{X}_i - \boldsymbol{X}_j|) \tag{2}$$

where $\boldsymbol{X}_i$ are the monomer coordinates and ℓ is the statistical bond length. The first term represents the connectivity of the polymer with harmonic springs of strength κ_{ij} introduced between any pair of connected monomers (which we denoted by $i \sim j$). It should be noted that we define a "monomer" in relation to the Kuhn length of the polymer. This beads-on-spring model therefore disregards more detailed bonded interactions, such as angular and torsional terms. For this reason, the model is not able to fully characterize atomistic differences between dendrimers with different chemical monomer units, such as local stiffness (however, as discussed in section 2, we can use different values of D to model more flexible dendrimers). However, as well as providing a more general description of co-dendrimer systems, it can also be used as a well-studied starting point[11,16,17,20] for more detailed atomistic simulations of specific co-dendrimer systems.

The second term in eq 2 represents pairwise nonbonded, i.e., van der Waals, interactions between monomers, and is also used to model solvent−solute interactions implicitly. We use the standard Lennard-Jones form of the potential

$$U_{ij}^{(LJ)}(r) = \begin{cases} +\infty, & r < d^{(0)} \\ U_{ij}^{(0)}\left(\left(\dfrac{d^{(0)}}{r}\right)^{12} - \left(\dfrac{d^{(0)}}{r}\right)^{6}\right) & r > d^{(0)} \end{cases} \tag{3}$$

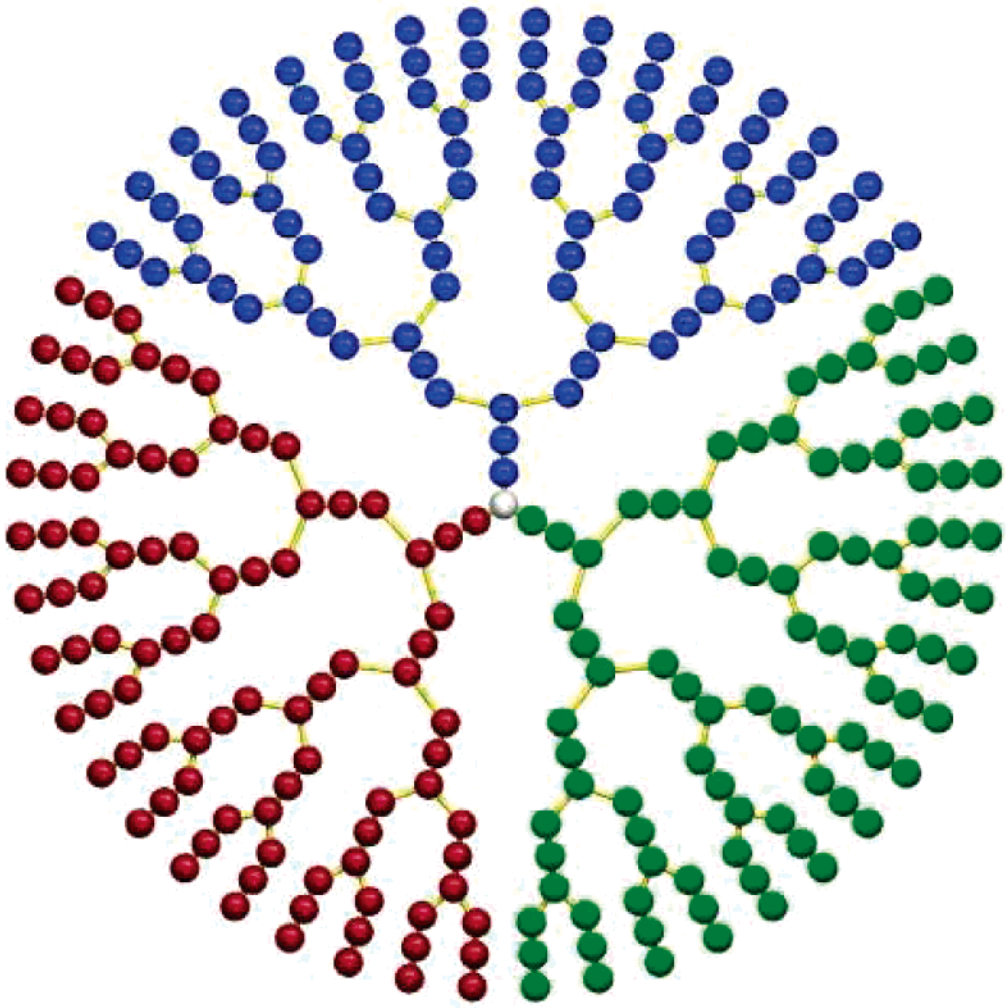

Figure 1. 2-Dimensional representation of the $F_0 = 3$ dendrons of a D3G4 dendrimer. To distinguish the monomers from separate dendrons the monomers (spheres of diameter $d = 1$) from each of the dendrons are colored with one of three colors (red, green, and blue).

where r is the distance between monomers i and j and $d^{(0)}$ corresponds to the monomer diameter, which is considered to be greater than or equal to the Kuhn length of the polymer. For the sake of convenience, we traditionally choose $d^{(0)} = 1$. Here $U_{ij}^{(0)}$ is the dimensionless strength of the "effective" Lennard-Jones interaction acting between monomers i and j. Note that this model contains a "hard sphere" form of the repulsions. The use of this model is computationally advantageous, since attempted MC steps which would cause an overlap of monomers can be automatically rejected, without evaluating the energy of the move. Note that, henceforth, we define all energies in units of k_BT and distances in units of $d^{(0)}$.

In amphiphilic copolymers, there are two types of monomers, hydrophobic (H) and polar (P). We model the behavior of these two types in aqueous solution with the following method incorporating the effect of the solvent into the Lennard-Jones term, as we have previously done for amphiphilic star copolymers.[16,17] We use the strength of the attractions between two hydrophobic monomers equal to a sufficiently large value, namely, $U_{HH}^{(0)} = 6k_BT$, corresponding to water being a poor solvent for hydrophobic monomers. The strength of the attractions between two polar monomers is then taken as being zero, $U_{PP}^{(0)} = 0$, corresponding to water being a good solvent for polar monomers which thus only experience hard sphere repulsions. Finally, we take the strength of the attractions between a hydrophobic monomer and a polar monomer as being the arithmetic mean of the two previous values, i.e., $U_{HP}^{(0)} = 3k_BT$. The latter condition, while physically simple and intuitive, is somewhat nontrivial to derive theoretically, but it has been previously well rationalized (see refs 17 and 20 and references therein).

3.1. Starting Conformations and Equilibration. The starting conformations used were those obtained from equilibrated simulations of the equivalent homodendrimers in either the good or the poor solvent.[11] For most of the systems, the amphiphilic solvent interaction terms were then introduced and the simulations were allowed to equilibrate. Since these simulations were only of single chain systems, equilibration was evaluated by monitoring the behavior of global observables such as the energy and the radius of gyration. Whenever possible, simulations were repeated a number of times using different random number seeds, to provide a larger ensemble. The process of "quenching" the solvent interactions term from the homopolymer terms to the amphiphilic terms can result in long-lived metastable conformations,[17] although this is not really a problem if the poor solvent homopolymer case is used for starting conformations. To ensure that this was not the case for our systems, we ran several additional representative

simulations, wherein the solvent interaction terms were slowly "annealed" from the homopolymer terms, in steps of, e.g., $0.2k_BT$, with extensive equilibration between each step. The resulting conformations were then compared with the equivalent "quenched" simulations in terms of the snapshots and observables discussed in this paper. Differences were only observed for some of the largest outer-H systems. For these co-dendrimers, we did find, in some members of the ensemble, long-lived metastable states, when quenching from the good solvent, equivalent to those found for amphiphilic star copolymers.[17] However, these were not observed when quenching from the poor solvent conformations. For some of the larger systems, we also carried out simulations using high energy, randomized globules of N monomers as starting conformations. We refer to these starting conformations as "frustrated globules', and we will discuss them further in section 4.3.

After reaching equilibrium, typically a large number of statistical measurements were performed. To ensure statistical independence of sampling, each consecutive measurement was separated by a large number of Monte Carlo sweeps (MCS). The number of MCS required between each measurement, was calculated by ensuring that the "statistical inefficiency" , s, of relevant observables tended toward 1, as described in ref 19. The mean value and error of sampling of an observable A are then given by the arithmetic mean

$$\langle A\rangle = (1/Q)\sum_{\gamma}^{Q} A_\gamma$$

and by

$$\pm\sqrt{(\Delta A)^2/Q}$$

respectively, where Q is the number of measurements (which are, in this case, statistically independent). If s is considerably greater than 1, consecutive measurements have some correlation, and obviously are no longer statistically independent. In this case, we calculate the errors of sampling via

$$\pm\sqrt{(\Delta A)^2 s/Q}$$

4. Simulation Results

MC simulations were carried out for both inner-H and outer-H co-dendrimers, with $D = 1$, 2 and $G = 1-7$ and $D = 3$, 4 and $G = 1-6$. In this section, we present the results from these simulations. Also, we have considered some representative examples of binary core co-dendrimers, which we will discuss briefly in section 4.4.

4.1. Asphericity Characteristics. First, let us consider the asphericities of these systems. As before,[21] we will define the nonaveraged *shape tensor*

$$Q^{\alpha\beta}(\boldsymbol{X}i) = \frac{1}{2N^2}\sum_{ij,i\neq j}(X_i^\alpha - X_j^\alpha)(X_i^\beta - X_j^\beta) \qquad (4)$$

which is related to the inertia tensor $I^{\alpha\beta} = \delta^{\alpha\beta}\,\mathrm{Tr}\,Q - Q^{\alpha\beta}$ in the case when all monomers have equal masses. In this case, $\alpha,\beta = 1$, 2, 3 (corresponding to the x, y and z Cartesian coordinates). If the instantaneous shape is nonspherical, then there should be some distinction between the three axes, and hence, we can obtain information about the shape from this matrix.

Let us then introduce the traceless tensor $\hat{Q}^{\alpha\beta} = Q^{\alpha\beta} - {}^1/_3\,\delta^{\alpha\beta}\,\mathrm{Tr}\,Q$ and the "mean" value of the eigenvalues $\bar{q} \equiv {}^1/_3\,\mathrm{Tr}\,Q$, where the trace of Q coincides with the nonaveraged (i.e., instantaneous) squared radius of gyration, namely: $\mathrm{Tr}\,Q = \sum_{a=1,2,3} q^{(a)} = 3R_g^2$.

One can now study the mean[2] ratios of the eigenvalues of the Q matrix

$$\lambda^{(a)} = \left\langle \frac{q^{(a)}}{\mathrm{tr}\,Q}\right\rangle = \left\langle \frac{q^{(a)}}{3\bar{q}}\right\rangle, \sum_{a=1,2,3}\lambda^{(a)} = 1 \qquad (5)$$

(We cannot just naively average Q over the whole ensemble, since the axes would then become symmetrical due to rotation. However, we should first sort the three eigenvalues in order of their magnitude for each measurement, and then average these sorted eigenvalues over all measurements.) One can consider the three λ values as corresponding to the "length", "width", and "breadth" of the polymer shape (divided by $3R_g^2$). If the polymer adopts perfectly spherical conformations, then all three of these values should be the same, and due to their normalization equal to ${}^1/_3$. Generally though, the λ values can distinguish between spherical and nonspherical conformations.

In addition, we can define the asphericity index

$$\mathscr{A}_3 = \langle A_3\rangle = \left\langle \frac{3}{2}\frac{\mathrm{Tr}\,\hat{Q}^2}{(\mathrm{tr}\,Q)^2}\right\rangle = \left\langle \frac{1}{6}\sum_{a=1,2,3}\frac{(q^{(a)} - \bar{q})^2}{\bar{q}^2}\right\rangle \qquad (6)$$

This observable is useful, since it can simply distinguish between spherical and nonspherical conformations with one value, i.e., 0 (sphere) $\leq \mathscr{A}_3 \leq 1$ (rodlike).

In Figure 2, we present the asphericity indices, A_3, for the (a) inner-H and (b) outer-H cases vs G, for $D = 1$, 2, and 3. Initially, with increasing G, for all the systems, the dendrimers adopt more spherical conformations; i.e., they demonstrate a similar trend to the homodendrimers (e.g., see Figure 3 in ref 11). However, after a certain number of generations ($G = 5$ or 6 for $D = 1$; $G = 4$ or 5 for $D = 2$, 3 (and also $D = 4$, although this is not illustrated here)), there is a significant increase in the asphericity. Although from this result it might be concluded that the trend of increasingly well-defined shapes with increasing G is somehow reversed, an analysis of the λ values from which the A_3 values are obtained, reveals that the dendrimers tend to adopt more elongated conformations for larger values of G. We illustrate this for the $D = 2$, cases in the insets of Figure 2. Initially, the three λ values all tend toward the same limit of ${}^1/_3$, hence adopting more spherical conformations. At a critical generation (which depends on D), the increasing steric congestion among the P monomers causes the dendrimers to adopt more elongated, almost cylindrical, conformations. We will discuss this phenomenon in section 4.3, but for now we note that these conformations are also well-defined, and $\lambda^{(2)}$ and $\lambda^{(3)}$ continue to converge, although $\lambda^{(1)}$ diverges from them, resulting in the large A_3 values. The elongated shape (where width $\approx$ breadth $\ll$ height) of the larger co-dendrimers is illustrated by the snapshots of the D2G7 cases in Figure 3. It can be seen that similar conformations are observed for both the inner-H and the outer-H topologies, albeit the outer-H dendrimers are "loopy micellar", rather than "micellar", using the same terminology as for star copolymers.[16,17]

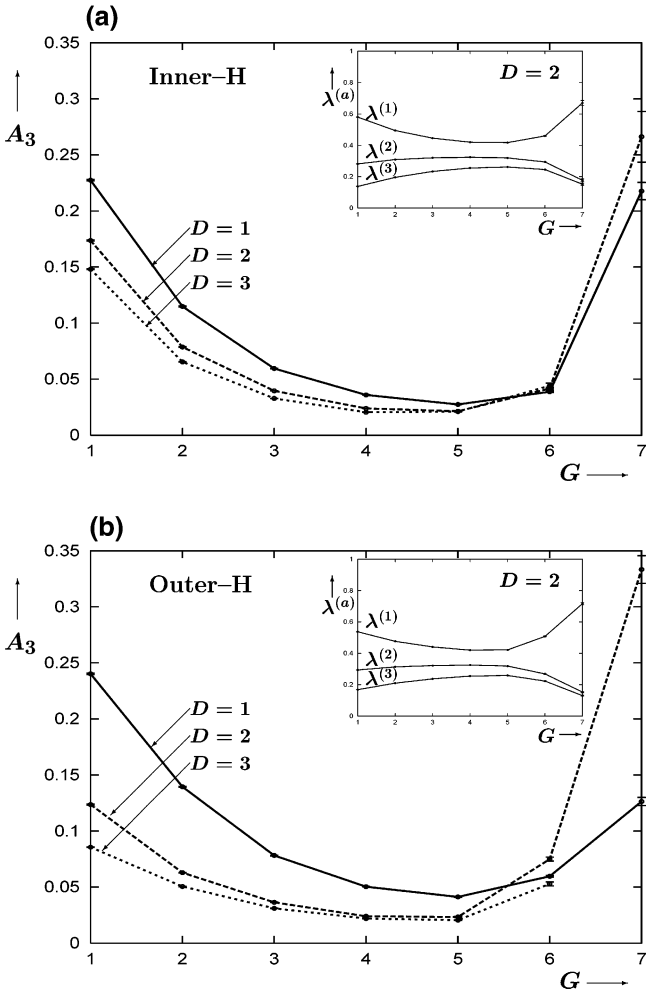

Figure 2. Asphericity indices, A_3, for (a) inner-H and (b) outer-H co-dendrimers of increasing generation. Errorbars are only noticeable for the higher generations. Insets correspond to the lambda values, $\lambda^{(a)}$, for $D = 2$.

Interestingly, if we use the monomer coloring of Figure 1 to distinguish the monomers from different dendrons, we find that there is not much mixing of the dendrons. Indeed, the elongated conformations in general tend to consist of two dendrons at bases of a cylinder (or symmetric ellipsoid) with the third being spread out in the middle. Our investigations do not suggest that there is any preferential distinction between which dendrons are involved as all three dendrons are chemically identical. These elongated shapes for the larger co-dendrimers were found in all members of the statistical ensemble, no matter which starting conformations were used. Some segregation of dendrons has been observed by Mansfield and Klushin for a homodendrimer in the good solvent.[22] However, in their case, the segregation was due to a radial force which was artificially applied to the terminal groups, to create initial starting conformations. For $D = 1$, the outer-H cases are not able to form as well-defined a micelle as the inner-H cases, as can be seen in Figure 4, and hence the outer-H dendrimers have greater A_3 values (i.e., are less spherical) than their inner-H counterparts. However, by increasing D, the H monomers are better able to backfold, forming more well-defined structures. Hence, for $D > 1$, the outer-H co-dendrimers are in fact more spherical, as is also found for amphiphilic star copolymers,[16] since the P monomers in the outer-H cases are more constrained and hence tend to reside closer to the center of mass, resulting in more spherical conformations.

From Figures 3 and 4, it appears that, qualitatively at least, both inner-H and outer-H are able to adopt quite similar conformations, especially for larger values of D and G. This is interesting, considering the entropic losses involved for the outer-H to form the "loopy micelle" equivalent of the inner-H "micelle". However, the fact that these loopy micelles are persistently obtained from the MC simulations itself offers further confirmation that these conformations are indeed the relevant lowest free energy structures. We can emphasize the similarities of both structures for large enough D and G, by examining the monomer density profiles of both systems.

4.2. Monomer Density Profiles. To compare the density profiles of the inner-H and outer-H D3G4 co-dendrimers, it is convenient to use the following rescaled dimensionless variables (as previously used by us to describe star copolymers[17])

$$\hat{\rho}_x(\hat{r}) \equiv \frac{4\pi\hat{r}^2\langle 3R_{g,x}{}^2\rangle\rho_x(\hat{r})}{N_{\mathrm{Tot}}} \tag{7}$$

$$\hat{r} \equiv \frac{r}{\langle 3R_{g,x}{}^2\rangle} \tag{8}$$

where the subscript x corresponds to the monomers of type x = H, P, or Tot, r is the distance from the center of mass, and ρ_x is the corresponding density profile, which should not be confused with the shell index or "span", ρ. The normalization condition for each of these functions is then simply

$$\int_0^\infty \mathrm{d}\hat{r}\ \rho_a(\hat{r}) = \frac{N_a}{N_{\mathrm{Tot}}} \tag{9}$$

In Figure 5, we plot these rescaled quantities for both the inner-H and outer-H cases. It can be seen that both dendrimers have similar plots. Indeed, the agreement between them is particularly interesting considering their substantially different connectivity, which we will emphasize in the next section. Still, they do not *exactly* overlap. In the inner-H case (dashed lines), the H monomers are slightly more localized and tend to lie closer to the center of mass. On the other hand, the P monomers are slightly more delocalized, and the tail extends farther for the inner-H case. This can be understood from the snapshots in Figures 3 and 4, since the P monomers in the outer-H case are looped back to the center of mass, confining them more than in the inner-H case. This also pulls the H monomers slightly away from the center of mass (as well as slightly shifting the center of mass).

We can also note that compared to star copolymers (see Figures 9 and 12 in ref 17), the P monomers are more localized. This occurs since the length of the P arms in stars is considerably longer than the length of the P blocks in the dendrimer; i.e., the P blocks in the co-dendrimer were of length $D = 3$ monomers, while the arms in ref 17 were 50 monomers long.

4.3. Distance of Monomers from the Center of Mass. Although, for large enough values of D and G, both the inner-H and outer-H topologies are able to adopt qualitatively similar conformations, with similar

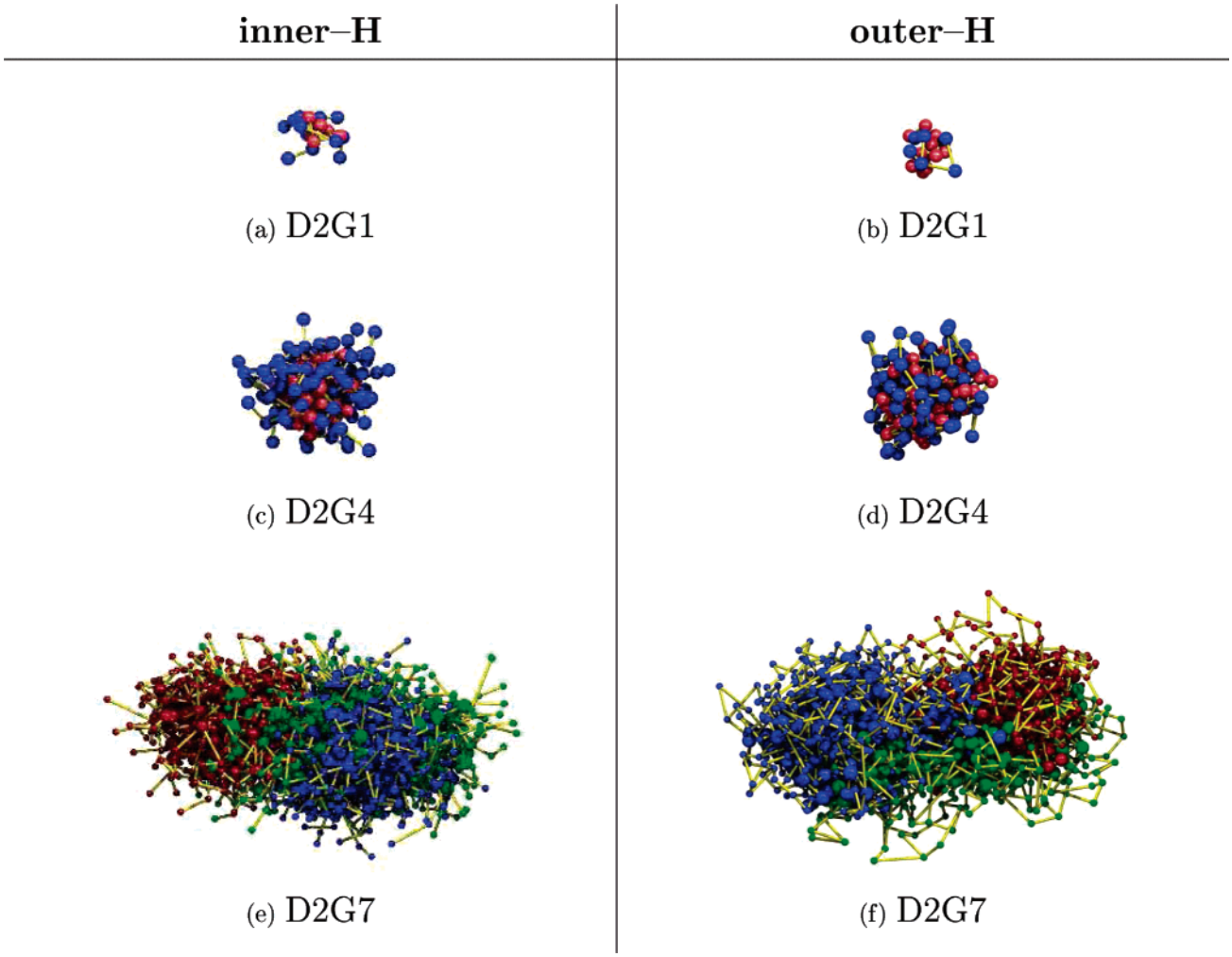

Figure 3. Typical snapshots, from Monte Carlo simulations, of various types of co-dendrimers with the same number of spacers ($D = 2$) between each branch point. Inner- and outer-H topologies are compared for three different degrees of branching, $G = 1$, 4, or 7. Unless otherwise stated, the monomers are colored red for H and blue for P. For visual clarity, the size of the spheres representing the polar monomers in the $G = 7$ cases have been reduced to $d = 0.5\sigma$. Also, to distinguish the monomers from separate dendrons, the monomer coloring of Fig. 1 is adopted for the $G = 7$ dendrimers.

density profiles, their internal structure is quite different. This can be emphasized by comparing the mean-squared (MS) distances of the monomers from their center of mass, $\langle R_{cm}^2 \rangle$, for both systems (see Figure 6), as well as the MS distances between consecutively bonded monomers, $D_{\rho-1,\rho}$ (see Figure 7).

We define these observables as follows,

$$\langle R_{cm}^2 \rangle(\rho) \equiv \frac{1}{3} \frac{\sum_{i \in \rho} \left\langle \left(\boldsymbol{X}_i - \frac{1}{N} \sum_j \boldsymbol{X}_j \right)^2 \right\rangle}{\sum_{i \in \rho}} \tag{10}$$

$$D_{(\rho-1,\rho)} \equiv \frac{1}{3} \langle (\boldsymbol{X}_{\rho-1} - \boldsymbol{X}_\rho)^2 \rangle \tag{11}$$

Considering Figure 6, it can be seen that for the inner-H cases the H monomers mostly reside close to the center of mass, as should be expected. It is important to emphasize that the H monomers farther along the span tend to be farther from the center of mass. Since there are more monomers in the higher generations, it is reasonable that they predominantly reside at greater distances from the center of mass, since this comprises a greater volume. This may be relevant in explaining the elongated conformations discussed in section 4.1 (D3G6 adopts elongated conformations and D3G5 is in the crossover region between spherical and elongated conformations). While we do not have a full quantitative explanation for these structures as yet, the following points should be important in understanding the phenomenon.

We have previously observed[11] that for the larger homodendrimers in the good solvent, the bonds near the center are quite stretched, to relieve the steric congestion of the outer generations (which contain a larger number of monomers and branch points), causing the development of cavities. Also for the outer generations there is a great deal of backfolding, which further relieves the steric congestion on the periphery. Obviously, the poor solvent cases correspond to compact globules, and the steric congestion here is superseded by the two-body attraction.

For the co-dendrimers, the P monomers should also suffer from the steric congestion, but the H monomers' bonds do not stretch to the same extent as the inner monomers' bonds of the good solvent homodendrimers, since energetically it is more favorable for them to form a fairly compact globule. This, in turn, forces the polar monomers of each generation closer together than they would be in the homodendrimer case, which should further exacerbate the steric congestion.

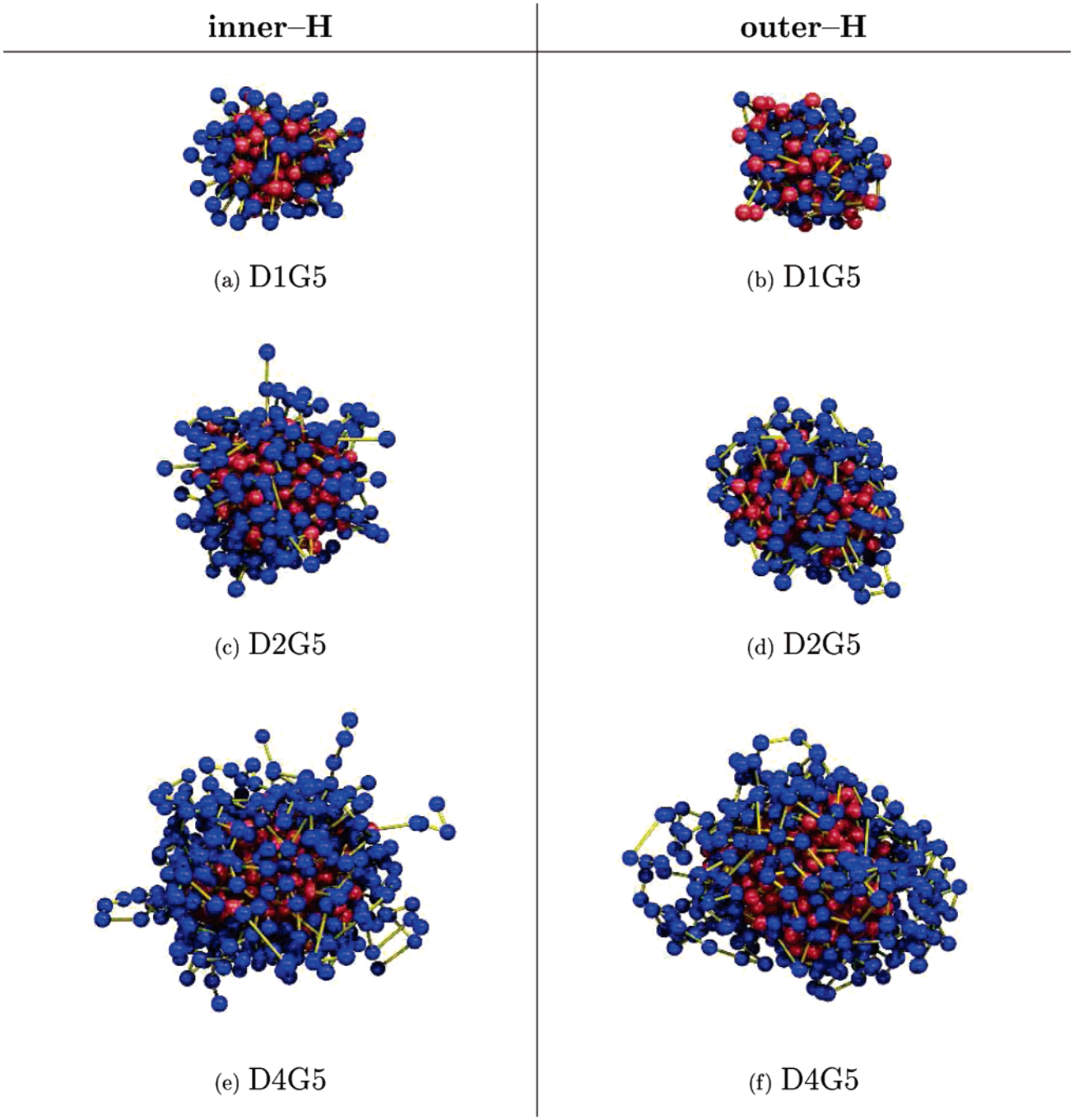

Figure 4. Typical snapshots, from Monte Carlo simulations, of various types of co-dendrimers with the same number of generations of branching ($G = 5$). Red and blue spheres correspond to H and P monomers, respectively. Inner- and outer-H topologies are compared with three different numbers of spacers between branch points, $D = 1$, 2 or 4.

For smaller generation co-dendrimers, the steric repulsion between the P blocks is not a problem for the spherical micelle (or loopy micelle) structures. However, as the number of P blocks increases, the steric congestion becomes problematic, and the larger dendrimers can no longer adopt these shapes. For instance, for the inner-H co-dendrimer, only the outermost generation is polar, residing in a relatively narrow layer around the compact H-globule. Deforming the spherical micelle into an aspherical one increases the entropy and reduces the steric congestion, as well as decreasing the energy of H−P interactions, due to a larger surface area. (In the present model the H−P contacts are favorable.) This, however, is opposed by an unfavorable energy gain of the hydrophobic core. The resulting aspherical shape will be more pronounced in larger dendrimers due to much higher steric congestion of the polar units. While the details of the loopy micelle structure formed for outer-H co-dendrimers will differ, the same argument should still apply as the highly interconnected P-blocks wrap around in a relatively narrow layer around the compact hydrophobic core. As we have seen in Figure 3, the asphericity of the micelles also results in dendron segregation, which is consistent with these “cigarlike” shapes.

One might speculate that star copolymers with a suitably large number of arms, f, should also demonstrate similar deviation from sphericity. To test this hypothesis, we carried out some simulations of many-arms star copolymers. In Table 1, we compare several different systems with similar total monomer numbers. Three co-dendrimer systems, which all demonstrate

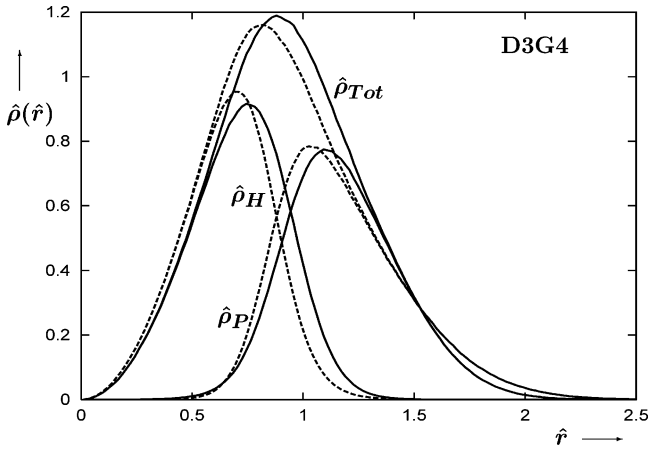

Figure 5. Rescaled dimensionless density, $\hat{\rho}(\hat{r})$, profiles for D3G4 co-dendrimers vs the dimensionless distance, $\hat{r}$. The densities are drawn for the H-monomers ($\hat{\rho}_H$), the P-monomers ($\hat{\rho}_P$), and all the monomers ($\hat{\rho}_{Tot}$). The continuous (dashed) lines correspond to the plots for the outer-H (inner-H) cases.

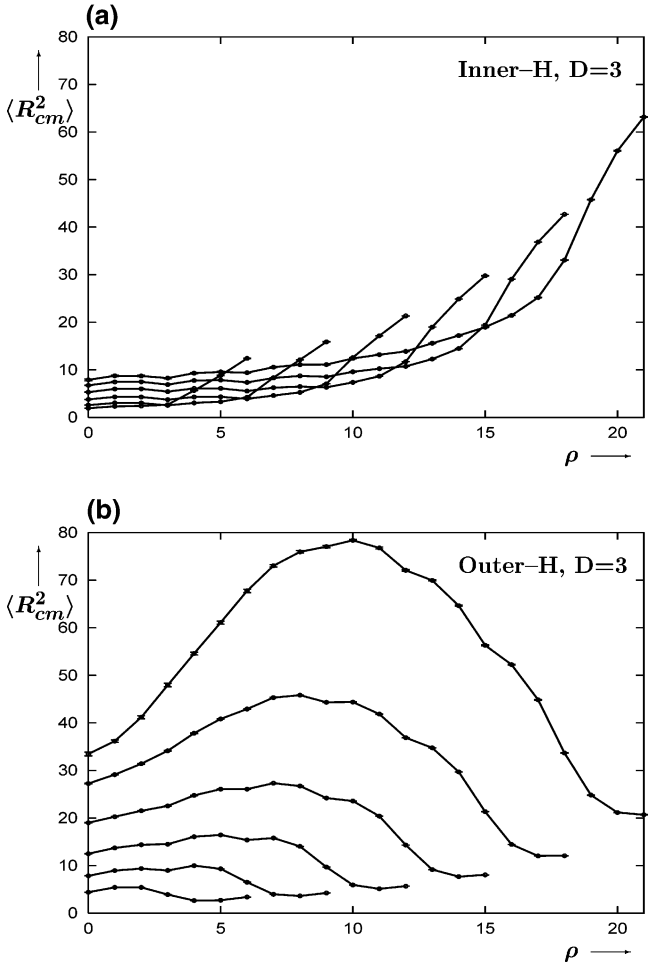

Figure 6. Mean-squared distance of monomers from the center of mass, $\langle R_{cm}{}^2\rangle$, along the span, ρ, for (a) inner-H and (b) outer-H, D3, co-dendrimers. Plots correspond to D3G1−D3G6, from bottom to top.

elongation are compared with an $f = 400$ arms star copolymer. We discuss here the inner-H case, but for comparison, we report the values of the D2G7 outer-H case in square brackets. All four systems have a similar number of monomers, N, and the length of the P blocks in the $f = 400$ star and the inner-H D2G7 are the same, i.e., two monomers.

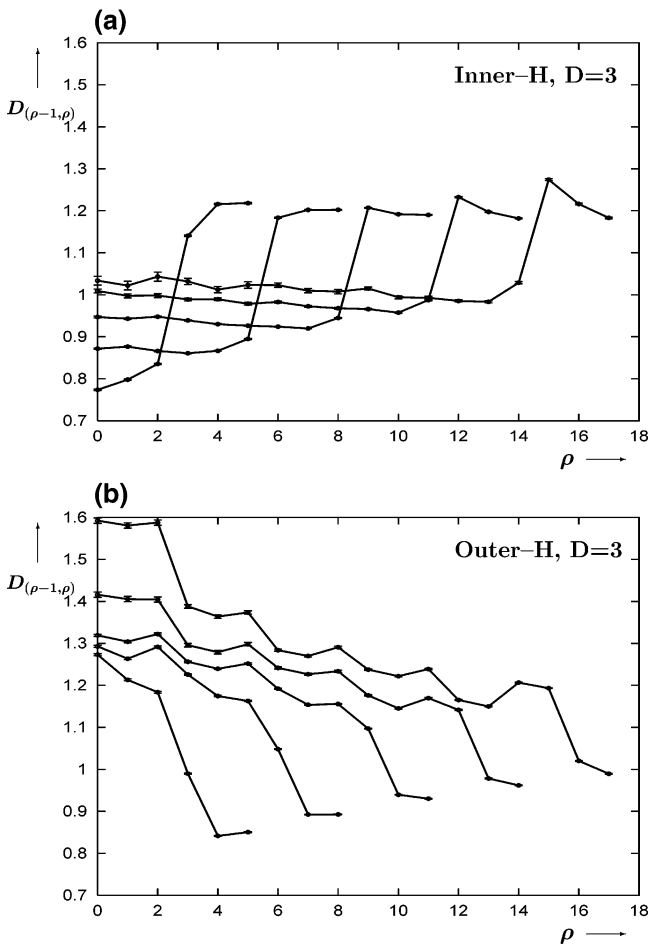

Figure 7. Plots of the mean-squared distance between consecutive monomers, $D_{(\rho-1,\rho)}$, i.e., MS bond length, along the span, ρ, for (a) inner-H and (b) outer-H, D3, co-dendrimers. Plots correspond to D3G1−D3G5, from bottom to top.

Table 1. Comparison of Various Shape-Related Observables for Several Different Related Systems

system	D2G7	D4G6	$f = 400$ star
N	1531	1525	1601
$\langle R_g{}^2\rangle$	56.58 [59.36]	47.12	39.59
A_3	0.266 [0.330]	0.051	0.0012
$\lambda^{(1)}$	0.671 [0.715]	0.480	0.353
$\lambda^{(2)}$	0.177 [0.154]	0.277	0.331
$\lambda^{(3)}$	0.152 [0.131]	0.243	0.316
$\langle H\rangle/k_BT$	−3467 [−3318]	−3706	−1490

[a] Column two is related to inner-H D2G7 co-dendrimers (the values in square brackets correspond to the outer-H equivalent); column three is related to inner-H D4G6 co-dendrimers; column four corresponds to an inner-H star copolymer[16,17] with $f = 400$ arms, each four monomers long, with $N_H = 0.5$, i.e., of composition HHPP. All of the systems were chosen, since they have similar values of N (first row). The MS values of the radii of gyration of the various systems are reported in the second row. The asphericity index, A_3, and the three lambda values, $\lambda^{(a)}$, are reported in rows 3−6. The final row illustrates the mean energy of the systems. Note that this is the mean energy of the system, and not the full Helmholtz free energy, $\mathcal{A} = \langle H\rangle - ST$, which would be more informative. Values are reported to the precision obtained from each set of simulation data.

From the table it can be seen, that compared to all three co-dendrimers, the star copolymers actually adopt highly spherical conformations. The main difference between stars and dendrimers is the number and distribution of the branch points. A star has a single branch point at the core monomer (which typically has a much greater degree of functionality, $f = 400$ in this

case). Dendrimers, on the other hand, have a greater number of branch points, and, in fact, the number of branch points increases along the span. Since the three dendrons are only connected by a single branch point, it appears that segregation at this branch point is the most economical way to minimize steric repulsion between the P blocks, since it reduces the number of bonds which must be stretched. This is also an explanation for the previously discussed cavities of high generation homodendrimers in the good solvent.[11] The differences between the star copolymers and the co-dendrimers appear to be sufficiently significant entropically to result in different shapes of these systems.

We have observed that increasing the steric repulsion between P blocks, by increasing D (since this increases the number of P monomers), appears to increase the degree of elongation somewhat. Indeed, for the $D = 1$ systems, elongation does not occur until after $G = 5$, while for the $D = 3$ and 4 systems, elongation is already noticeable for $G = 5$. It also seems, by comparing the two D2G7 systems in Table 1, that the outer-H topology is more elongated than the inner-H topology. It appears that the extra entropic constraints of the loopy micelle structures emphasize the degree of segregation.

One could argue that the initial conformations of the dendrimer used in the MC simulations could bias future conformations. For instance, if conformations of homodendrimers in the good solvent were used, then the initial proximity of the monomers in individual dendrons could result in the dendrons segregating first, before collapsing into a more compact globule or micelle, i.e., the simulation could be "funneled" through configuration space to a minimum, which may be only local. If the energy barriers between the various minima are high (which is likely for complex systems such as these), then it is feasible that the MC simulation would then be unable to locate any deeper minima in a reasonable time. To verify that this is not the case, we carried out additional simulations using initial conformations which did not have this bias. To achieve this, globular equilibrium conformations obtained from MC simulations of the equivalent homodendrimers in the poor solvent were modified by randomly swapping the monomer locations repeatedly, e.g., the Cartesian coordinates of monomers 3 and 172 could be replaced, although the connectivity between the monomer numbers would remain the same. Hence, monomer 3 would still be connected to monomers 2 and 4, although it would now be in the original location of monomer 172. When the monomer locations were suitably randomized, the resulting structures were referred to as "frustrated globules", since the bonds of all the monomers would be unrealistically stretched. The initial energies of these structures were very high, and the monomers belonging to each dendron are randomly located, hence removing any of the mentioned biases.

The results indicate that when frustrated globules are used as initial conformations, the monomers rapidly rearrange themselves to reduce bond stretching. This rearrangement reverts to the same conformations found using other initial conformations, i.e., the monomers in each dendron segregate before inter-dendron aggregation occurs.

Returning to the plots in Figure 6, we notice that the three last monomers along the span of the inner-H co-dendrimers, i.e., the P monomers, reside at a considerable distance from the center of mass, as well as

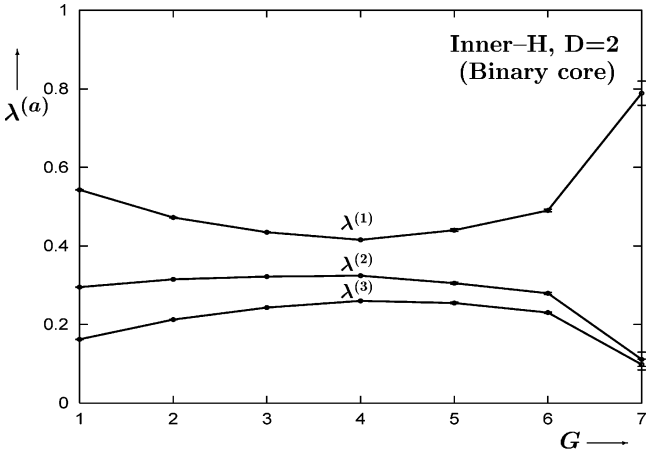

Figure 8. $\lambda^{(a)}$ values for inner-H, D2, co-dendrimers of increasing generation, as in the insets of Figure 2, only with a binary core.

appearing to "pull" some of the outer H monomers with them, i.e., the H monomers that are directly connected to the P monomers are pulled away to a certain extent from the rest of the H globule. This is more evident in Figure 7, where we plot the MS distance between consecutive monomers along the span, i.e., the MS bond lengths (as we did for the homodendrimers in ref 11). Here we observe that the bonds between the H and P monomers (i.e., the H monomers which act as the branch points for the outer P generation) and to a lesser extent, the bond between these H monomers and the H monomers they are connected to (i.e., the third and fourth last points on each plot, respectively) are both more stretched than the other H−H bonds.

In Figure 6b, we consider the outer-H equivalents. These plots are qualitatively similar to the equivalent plots obtained by our group for outer-H star copolymers (Fig. 11 in Ref. 17), in that the P monomers that are farthest away from both the H globule and the core monomer, i.e., the middle P generations, have the greatest distance from the center of mass, and both the core monomer and the H monomers are relatively close to the center of mass. However, in the co-dendrimers, the number of P monomers in the P-blocks (3 in this case) is smaller than in the stars (25 in Ref. 17). Also, it can be seen that the branch points (i.e., every fourth monomer) tend to be slightly closer to the center of mass than the other monomers.

In Figure 7b, we consider the MS bond lengths of the outer-H dendrimers. The plots have some similarity to those for good solvent homodendrimers (see Figures 7, 8, and 9 in Ref. 11). As with the homodendrimers, the inner generations are most highly stretched, with the stretching decreasing along the span. The branch points (every fourth monomer) are also more stretched than interior monomers. The interior P monomers are indeed considerably stretched, compared with the P monomers of Figure 7a, since they adopt more constrained loopy micelles. However, like their inner-H counterparts, the H−P bonds are more highly stretched than the H−H bonds.

4.4 Binary core dendrimers. As we mentioned in section 2, many of the currently synthesized amphiphilic co-dendrimers contain a binary core. Hence, it is of interest to see how this topology affects the conformations adopted. In Figure 8, we plot the λ eigenvalues for the inner-H, D2, co-dendrimers of increasing generation, as in the insets of Figure 2 (except for the presence

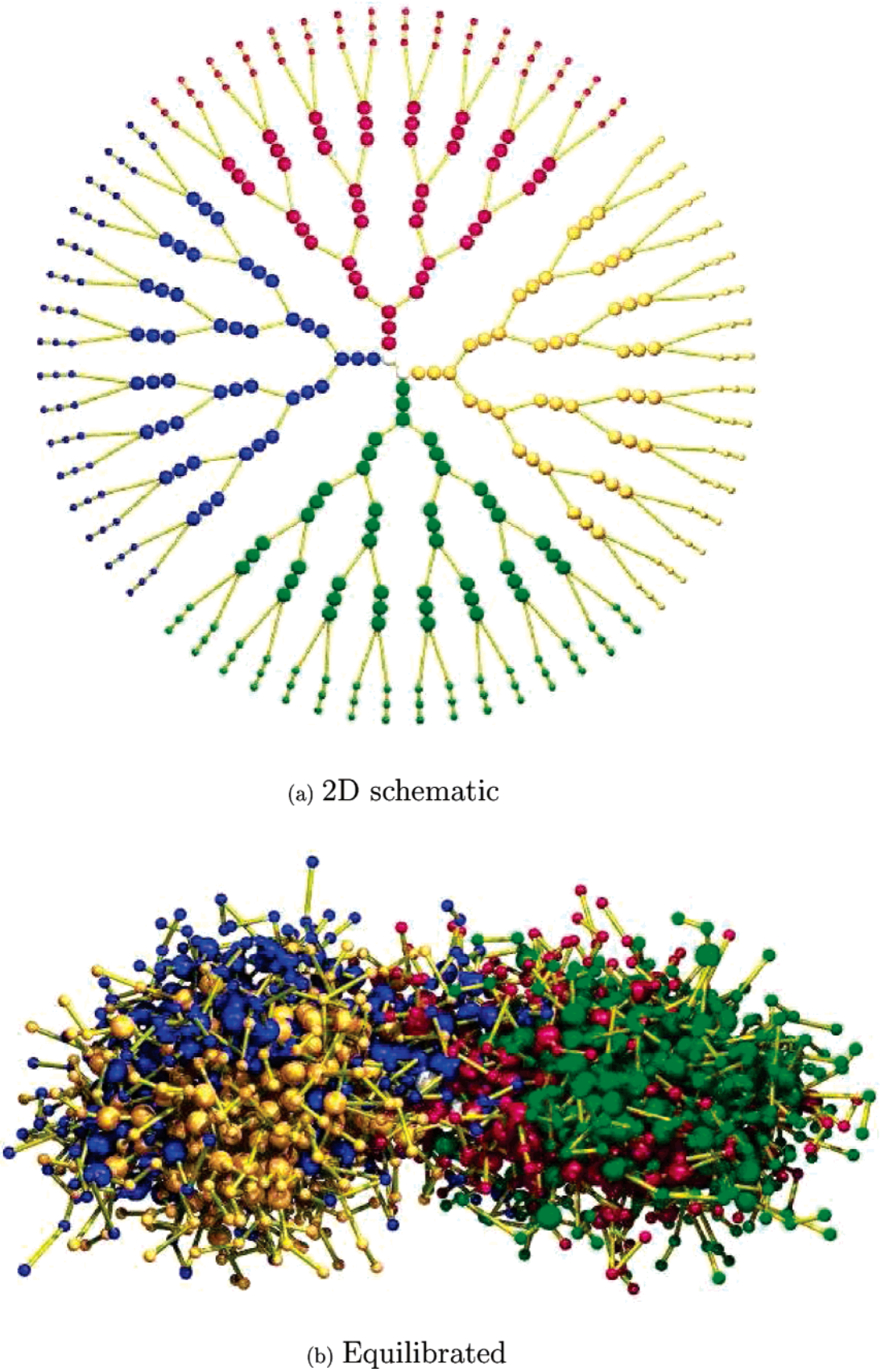

Figure 9. (a) Schematic representation of an inner-H D3G4 binary core co-dendrimer. (b) Typical snapshot, from MC simulations, of an inner-H D2G7 binary core co-dendrimer. For visual clarity, the size of the spheres representing the polar monomers have been reduced to $d = 0.5\sigma$, as in Fig. **3**. Also, to distinguish the monomers from separate dendrons, the monomer coloring of part a is also adopted for part b.

of a binary core). Comparing Figure 8 and the inset of Figure 2a, we find they are quite similar. The binary core shapes appear to be slightly more well-defined than their single core counterparts, i.e., slightly more spheri-

cal for small generations, and slightly more elongated for the higher generations. However, this is probably due to the larger number of monomers in the binary core case. For instance, the $G = 0$ generation has 4 branch points in the binary core case, while it only has 3 branch points for the single core case.

Since the elongated structures observed in Figure 3 for the D2G7 single core cases appeared to involve segregation of the three dendrons, the mixing of the dendrons in the binary core case is of interest. In Figure 9, a typical snapshot of an inner-H, D2G7, binary core co-dendrimer is presented. It appears that for the binary core, segregation also occurs, although in this case, pairs of dendrons are separated from each other in conformations reminiscent of "dumbbells". Interestingly, in this snapshot the dendrons opposite each other in the core align together, rather than those adjacent to each other.

5. Conclusions

In this paper, we have discussed the conformations adopted by two types of amphiphilic co-dendrimers. In one type, "outer-H", the outer generation consisted of only hydrophobic (H) monomers and the other generations consisted of polar (P) monomers. The opposite type was referred to as "inner-H". As for amphiphilic star copolymers,[16,17] for most of the systems, micelles and loopy micelles were formed for the inner-H and outer-H cases, respectively. We considered trifunctional co-dendrimers, which could be treated as comprising three dendrons attached to a single core monomer.

Although the inner-H dendrimers had more well-defined conformations than their outer-H counterparts for $D = 1$, since considerable bond-stretching was required by the P monomers to form the loopy micelles, for greater values of D, the outer-H dendrimers were able to form quite well-defined loopy micelles. In fact, since the P monomers were more constrained in the loopy micelles, the outer-H dendrimers adopted more spherical conformations than their inner-H equivalents for $D > 1$.

For high generations ($G > 4$ or 5), both types of co-dendrimer were found to adopt elongated conformations, rather than the spherical conformations found for the smaller co-dendrimers, and the homodendrimers. This elongation appeared to involve a segregation of the three dendrons in the co-dendrimers to form "cigar-like", cylindrical (or symmetric ellipsoidal) structures with consist of two dendrons at bases with the third being spread out in the middle. It was suggested that this was related to the increasing steric congestion among the P monomers. However, star copolymers with many ($f = 400$) short arms, were still found to form spherical structures, even though both systems have similar total number of monomers. Hence, the elongation of the co-dendrimers also seems related to the much higher density of branch points in the outer generations and much stronger steric repulsion of the polar units. It was also found that increasing the number of spacers between branch points partially decreased the critical number of generations necessary for elongation, suggesting that both effects contribute to the elongation. Outer-H topologies were found to be more elongated than their inner-H topologies.

This elongation of co-dendrimer micelles appears to be due to a compromise between an entropy gain and reduced steric congestion of the polar monomers accompanied by a favorable energy loss for the H−P contacts due to a larger surface area, and an unfavorable energy gain for the hydrophobic core. The quantitative details of these relative contributions to the thermodynamics of elongation seems to be a nontrivial question worthy of further rationalization.

Perhaps this matter could be better elucidated by theoretical means. However, given the anisotropic nature of these micelles, constructing a sufficiently accurate mean-field theory is by no means a simple task.

Although we mainly discussed the case of trifunctional dendrimers, we also briefly considered the conformations of dendrimers with binary cores, i.e., two trifunctional core branch points attached to each other. The binary core structures appear to be slightly more well-defined than their single core counterparts, i.e., slightly more spherical for small generations, and slightly more elongated for the higher generations. This is likely to be due to the larger number of monomers in the binary core case. Segregation of dendrons also occurs for the binary core, although in this case, pairs of dendrons are separated from each other in conformations reminiscent of "dumbbells", rather than the "cigar-like" conformations observed for the single core co-dendrimers.

The amphiphilic co-dendrimers studied here are of general interest for drug delivery applications since they have been found to form unimolecular micelles.[2,4,6,7] We hope that the novel well-defined cigar-like and dumbbell-like shapes described in this paper may also find applications as building blocks for supramolecular chemistry.[9]

Acknowledgment. We are grateful to Professor Giuseppe Allegra, Professor Fabio Ganazzoli, and Dr. Guido Raos for interesting discussions on the subject. We also thank Gillian Flanagan, Marese O'Brien, and Tina O'Farrell for their work on gaining preliminary insights into the problem during the course of their undergraduate projects.

References and Notes

(1) Matthews, O. A.; Shipway, A. N.; Stoddart, J. F. *Prog. Polym. Sci.* **1998**, *23*, 1. Grayson, S. M.; Fréchet, J. M. J. *Chem. Rev.* **2001**, *101*, 3819. Bosman, A. W.; Janssen, H. M.; Meijer, E. W. *Chem. Rev.* **1999**, *99*, 1665. Newkome, G. R.; Moorefield, C. N.; Vögtle, F. *Dendritic Molecules: Concepts, Synthesis, Perspectives*; Verlag-Chemie: Weinheim, Germany, 1996. Tomalia, D. A.; Naylor, A. M.; Goddard, W. A., III. *Angew. Chem., Int. Ed. Engl.* **1990**, *29*, 138. Mekelburger, H. B.; Jaworek, W.; Vögtle, F. *Angew. Chem., Int. Ed. Engl.* **1992**, *31*, 1571.

(2) Liu, M.; Fréchet, J. M. J. *Pharm. Sci. Technol. Today* **1999**, *2*, 393.

(3) Twyman, L. J.; Beezer, A. E.; Esfand, R.; Hardy, M. J.; Mitchell, J. C. *Tetrahedron Lett.* **1999**, *40*, 1743.

(4) Liu, M.; Kono, K.; Fréchet, J. M. J. *J. Controlled Release* **2000**, *65*, 121.

(5) Allen, C.; Maysinger, D.; Eisenberg, A. *Colloids Surf., B* **1999**, *16*, 3. Kim, S. Y.; Shin, I. G.; Lee, Y. M.; Cho, C. S.; Sung, Y. K. *J. Controlled Release* **1998**, *51*, 13. Ryu, J.-G.; Jeong, Y.-I.; Kim, Y.-H.; Kim, I.-S.; Kim, D.-H.; Kim, S.-H. *Bull. Kor. Chem. Soc.* **2001**, *22*, 467. Förster, S.; Antonietti, M. *Adv. Mater.* **1998**, *10*, 195.

(6) Hawker, C. J.; Wooley, K. L.; Fréchet, J. M. J. *J. Chem. Soc., Perkin Trans.* **1993**, *1*, 1287.

(7) Piotti, M. E.; Rivera Jr., F.; Bond, R.; Hawker, C. J.; Fréchet, J. M. J. *J. Am. Chem. Soc.* **1999**, *121*, 9471. Cooper, A. I.; Londono, J. D.; Wignall, G.; McClain, J. B.; Samulski, E. T.; Lin, J. S.; Dobrynin, A.; Rubinstein, M.; Burke, A. L. C.; Fréchet, J. M. J.; DeSimone, J. M. *Nature (London)* **1997**, *389*, 368. Stevelmans, S.; van Hest, J. C. M.; Jansen, J. F. G. A.; van Boxtel, D. A. F. J.; de Brabander-van den Berg, E. M. M.; Meijer, E. W. *J. Am. Chem. Soc.* **1996**, *118*, 7398.

Schenning, A. P. H. J.; Elissen-Román, C.; Weener, J.-W.; Baars, M. W. P. L.; van der Gaast, S. J.; Meijer, E. W. *J. Am. Chem. Soc.* **1998**, *120*, 8199. Sayed-Sweet, Y.; Hedstrand, D. M.; Spindler, R.; Tomalia, D. A. *J. Mater. Chem.* **1997**, *7*, 1199. Pan, Y.; Ford, W. T. *Macromolecules* **1999**, *32*, 5468.

(8) Watkins, D. M.; Sayed-Sweet, Y.; Klimash, J. W.; Turro, N. J.; Tomalia, D. A. *Langmuir* **1997**, *13*, 3136.

(9) Zeng, F.; Zimmerman, S. C. *Chem. Rev.* **1997**, *97*, 1681.

(10) Moore, J. S. *Acc. Chem. Res.* **1997**, *30*, 402.

(11) Timoshenko, E. G.; Kuznetsov, Yu. A.; Connolly, R. *J. Chem. Phys.* **2002**, *117*, 9050.

(12) Percec, V.; Chu, P.; Ungar, G.; Zhou, J. *J. Am. Chem. Soc.* **1995**, *117*, 11441.

(13) Schlüter, A.-D.; Claussen, W.; Freudenberger, R. *Macromol. Symp.* **1995**, *98*, 475.

(14) Trollsås, M.; Hedrick, J. L. *J. Am. Chem. Soc.* **1998**, *120*, 4644. Hedrick, J. L.; Trollsås, M.; Hawker, C. J.; Atthoff, B.; Claesson, H.; Heise, A.; Miller, R. D.; Mercerreyes, D.; Jérôme, R.; Dubois, Ph. *Macromolecules* **1998**, *31*, 8691. Ishizu, K.; Takeda, H.; Furukawa, T. *Polymer* **2000**, *41* 8299. Ishizu, K.; Takeda, H. *Eur. Polym. J.* **2001**, *37* 2073.

(15) Ganazzoli, F.; La Ferla, R.; Terragni, G. *Macromolecules* **2000**, *33*, 6611. Ganazzoli, F.; La Ferla, R.; Raffaini, G. *Macromolecules* **2001**, *34*, 4222.

(16) Connolly, R.; Timoshenko, E. G.; Kuznetsov, Yu. A. *J. Chem. Phys.* **2003**, *119*, 8736.

(17) Ganazzoli, F.; Kuznetsov, Yu. A.; Timoshenko, E. G. *Macromol. Theory Simul.* **2001**, *10*, 325.

(18) Metropolis, N.; Rosenbluth, A. W.; Rosenbluth, M. N.; Teller, A. H.; Teller, E. *J. Chem. Phys.* **1953**, *21*, 1087.

(19) Allen, M. P.; Tildesley, D. J. *Computer Simulations of Liquids*, 1st ed.; Clarendon Press: Oxford, England, 1987.

(20) Timoshenko, E. G.; Kuznetsov, Yu. A. *J. Chem. Phys.* **2000**, *112*, 8163.

(21) Timoshenko, E. G.; Kuznetsov, Yu. A.; Connolly, R. *J. Chem. Phys.* **2002**, *116*, 3905.

(22) Mansfield, M. L.; Klushin, L. I. *Macromolecules* **1993**, *26*, 4262.

MA049638B